

The metallochaperone Atox1 plays a critical role in perinatal copper homeostasis

Iqbal Hamza*, Anja Faisst†, Joseph Prohaska‡, Joseph Chen*, Peter Gruss†, and Jonathan D. Gitlin*§

*Department of Pediatrics, Washington University School of Medicine, St. Louis, MO 63110; †Department of Molecular Cell Biology, Max Planck Institute, 37077 Gottingen, Germany; and ‡Department of Biochemistry and Molecular Biology, University of Minnesota Duluth School of Medicine, Duluth, MN 55812

Edited by William S. Sly, Saint Louis University School of Medicine, St. Louis, MO, and approved April 3, 2001 (received for review February 5, 2001)

Copper plays a fundamental role in the biochemistry of all aerobic organisms. The delivery of this metal to specific intracellular targets is mediated by metallochaperones. To elucidate the role of the metallochaperone Atox1, we analyzed mice with a disruption of the *Atox1* locus. *Atox1*^{-/-} mice failed to thrive immediately after birth, with 45% of pups dying before weaning. Surviving animals exhibited growth failure, skin laxity, hypopigmentation, and seizures because of perinatal copper deficiency. Maternal *Atox1* deficiency markedly increased the severity of *Atox1*^{-/-} phenotype, resulting in increased perinatal mortality as well as severe growth retardation and congenital malformations among surviving *Atox1*^{-/-} progeny. Furthermore, *Atox1*-deficient cells accumulated high levels of intracellular copper, and metabolic studies indicated that this defect was because of impaired cellular copper efflux. Taken together, these data reveal a direct role for *Atox1* in trafficking of intracellular copper to the secretory pathway of mammalian cells and demonstrate that this metallochaperone plays a critical role in perinatal copper homeostasis.

Copper is a transition element that plays an essential role in the metabolic pathways required for cellular respiration, iron homeostasis, pigment formation, neurotransmitter production, peptide biogenesis, connective tissue biosynthesis, and antioxidant defense (1). Recognition of the inherited disorders of copper transport, Menkes and Wilson disease, dramatically underscored both the essential need for copper and the toxicity of this metal (2). Characterization of the molecular genetic basis of these disorders has provided the opportunity to elucidate the molecular mechanisms of cellular copper metabolism, including the recent identification in *Saccharomyces cerevisiae* of a family of cytoplasmic proteins termed metallochaperones, proposed to play a role in intracellular copper trafficking (3, 4).

Genetic and biochemical studies in yeast suggest that metallochaperones function to protect copper from intracellular scavenging while facilitating the appropriate partnerships with specific cupro-protein targets (5). The yeast metallochaperone Atx1 plays a role in copper delivery to the secretory pathway in this organism via interaction with the copper transport ATPase Ccc2 (6–8). Structural and functional analysis of the mammalian Atx1 homologue, ATOX1 (or HAH1), indicates that this protein interacts with the Menkes and Wilson copper-transporting ATPases located in the *trans*-Golgi network of cells (9, 10). Analysis of Wilson disease-associated mutations in the amino terminus of the Wilson ATPase suggests a critical role for ATOX1–ATPase interaction in hepatocyte copper homeostasis (10). Nevertheless, despite these experiments in yeast and in mammalian cell lines, the physiologic role of ATOX1 in mammals remains to be determined. This current study was undertaken to elucidate the function of ATOX1 in mammalian cells and to examine its role in cellular copper homeostasis by using a genetic mouse model.

Materials and Methods

Generation of *Atox1*^{-/-} Null Mice. R1 embryonic stem cells were cultured and electroporated, and neomycin-resistant clones as-

ayed positive for β -galactosidase activity were aggregated with morula-stage embryos to generate chimeric mice as described (11). The genomic structure of mouse *Atox1* has been reported (12), and Southern blot and 5'-rapid amplification of cDNA ends analysis of genomic DNA from these embryonic stem cells confirmed the presence of the β -geo gene trap at the *Atox1* locus. Chimeric mice were mated to CD-1 animals to obtain germ-line transmission of the disrupted *Atox1* allele. Mice heterozygous for the trapped allele were backcrossed six times (N6) to C57BL/6 mice and intercrossed seven times (F7). All subsequent analyses were performed with N6F7 generation mice. All mice were housed at the Washington University School of Medicine Vivarium under a 12-h light/12-h dark cycle. Food and water were provided ad libitum, and all care was given in compliance with National Institutes of Health guidelines on the use of laboratory and experimental animals.

Genotyping and Analysis of Mice. Southern blot of wild-type (wt) and mutant genomic DNA digested with multiple restriction enzymes and analyzed with a 5' *Atox1* probe confirmed that the β -geo insertion is at the *Atox1* locus. Southern blot with a neomycin DNA probe revealed a single insertion of the β -geo cassette at the *Atox1* locus. PCR was performed by two-allele, three-primer analysis by using genomic DNA template prepared from tail clips or embryonic tissues. PCR of the wt allele with primers (available on request) resulted in a 700-bp product, whereas PCR of the mutated allele resulted in a 1,300-bp fragment. Initial PCR results were verified by Southern analysis of genomic DNA from the same mice. RNA blot analyses were performed from total RNA isolated from E12.5 embryonic fibroblasts and hybridized with *Atox1* or 18S DNA probe using UltraHyb (Ambion, Austin, TX). Immunoblot analyses were performed by using ATOX1 antisera and chemiluminescent techniques (12). No detectable Atox1 protein was observed in multiple tissues obtained from surviving *Atox1*^{-/-} animals. Growth was monitored by weighing animals starting from P0 to P30 every 24 h. Hypothermia was evaluated by the ability of mice to maintain body temperature at 4°C within a 3-h period by using a rectal digital thermometer. Milk spots were determined by examining the stomach contents of dissected P1 pups. For blood values, P1 pups were decapitated, and blood drawn into heparinized capillary tubes was used immediately to obtain hematocrits, sodium, and glucose values.

Radiolabeled Copper Studies. Placental copper transport studies were initiated in E14.5 timed pregnant dams by i.v. tail injection of 1 mCi of ⁶⁴Cu that was preequilibrated with 50 μ g of copper

This paper was submitted directly (Track II) to the PNAS office.

Abbreviations: COX, cytochrome oxidase; wt, wild type; MEFs, mouse embryonic fibroblasts.

See commentary on page 6543.

§To whom reprint requests should be addressed. E-mail: gitlin@kids.wustl.edu.

The publication costs of this article were defrayed in part by page charge payment. This article must therefore be hereby marked "advertisement" in accordance with 18 U.S.C. §1734 solely to indicate this fact.

(chloride salt) in 100 μ l of saline (13, 14). Twenty-four hours later, the individual placenta and embryo were dissected from the maternal tissues and rinsed three times with PBS before quantifying the amount of tissue ^{64}Cu incorporation in a Packard Gamma Counter. Each data point was calculated as the ratio of the amount of ^{64}Cu (cpm) retained within that tissue to the total amount of ^{64}Cu (cpm) injected into the mother. For cell culture experiments, mouse embryonic fibroblasts (MEFs) from E12.5 embryos were isolated and cultured in DMEM with 10% FCS as described (15). After the first passage, the MEFs were genotyped by PCR analysis. Mouse fibroblast cell lines (802-5 and 802-1) were cultured as described (16). For copper retention studies, 2×10^5 cells were allowed to adhere onto 35-mm Petri dishes before incubation for 68 h with 8×10^6 cpm of ^{64}Cu in culture medium. The cells were then washed three times with ice-cold PBS, lysed with PBS containing 1% SDS, and analyzed for ^{64}Cu retention by using the gamma counter. For copper uptake and efflux experiments, 8×10^6 cpm of ^{64}Cu was premixed with 200 nM copper (chloride salt) and 400 nM L-histidine (Sigma) for 1 h at 37°C in serum-free OPTIMEM (Life Technologies, Grand Island, NY). Copper uptake was initiated by incubating MEFs with 200 nM ^{64}Cu per 4×10^4 cells at 37°C, and at different time points the uptake was terminated by rapid aspiration of ^{64}Cu media and incubation in an ice-water bath. For efflux studies, cells were pulsed with 200 nM ^{64}Cu for 1 h as described above, followed by three quick rinses with prewarmed PBS to remove any residual copper, and then incubated with prewarmed OPTIMEM alone for several chase periods. Cells were harvested at different time intervals and processed for quantification as described for copper retention.

Copper and Enzyme Activity Measurements. Copper concentrations and enzymatic activities were measured from wt and *Atox1*^{-/-} P2 organs obtained from 5 litters (38 pups) of *Atox1*^{+/-} matings. Total tissue copper content was measured by acid digestion of tissue and atomic absorption spectrophotometry (17). Cytochrome *c* oxidase activity was measured spectrophotometrically on whole homogenates by monitoring loss of ferrocytochrome *c* (17). Tyrosinase activity was measured in whole-skin homogenates as an in-gel dopa oxidase assay as described (18). Succinate dehydrogenase activity was measured by the reduction of 2,6-dichlorophenol indophenol at 600 nm as described (19). Limited tissue prohibited direct assay of lysyl oxidase or dopamine monoxygenase activities.

Results

To determine the physiologic role of ATOX1, we characterized a mouse *Atox1* locus that was disrupted by gene-trap insertion of a β -galactosidase-neomycin marker (β -geo) between the first and second exons of one allele of *Atox1* in embryonic stem cells (Fig. 1A) (12, 20). Germ-line chimeras derived from morula aggregation with the mutated cells were used to obtain heterozygous *Atox1*^{+/-} mice that were bred to homozygosity and ascertained by Southern blot analysis of mouse genomic DNA by using a 5' *Atox1*-specific probe (Fig. 1B) and a neomycin DNA probe (data not shown). Analysis of mouse fibroblasts from E12.5 embryos indicated that the β -geo insertion resulted in an *Atox1* null allele, as no *Atox1* mRNA nor protein was detected in *Atox1*^{-/-} homozygous animals based on RNA blots and immunoblots, respectively (Fig. 1C and D).

Analysis of staged offspring from *Atox1*^{+/-} matings showed the expected Mendelian ratio until birth, but revealed a growth retardation phenotype in *Atox1*^{-/-} neonatal mice that was apparent in most pups by postnatal day 3 (P3) (Fig. 2A). Organ weight to body length comparison of mutant and wt littermates indicated that this growth impairment was symmetrical (data not shown). Despite normal sucking behavior, the presence of milk spots and normal red cell hemoglobin (hematocrit; +/+ 37.83 \pm

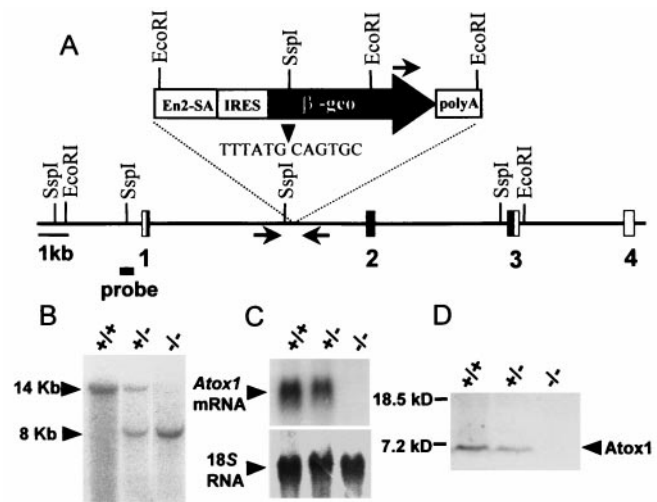


Fig. 1. Generation of the *Atox1* null allele. (A) The genomic locus of the mouse *Atox1* gene disrupted by the promoterless β -galactosidase-neomycin (β -geo) cassette. The relevant restriction sites, location of the β -geo insertion (arrowhead) between exons 1 and 2, the 5' probe for Southern analysis (horizontal bar), and location of sequences used as primer sets for genotyping (horizontal arrows) are indicated (En2-5A, *engrailed* 2 splice acceptor site; IRES, internal ribosome entry site). (B) Southern blot analysis of genomic DNA digested with *EcoRI* from *Atox1*^{+/+}, *Atox1*^{+/-}, and *Atox1*^{-/-} embryos and probed with the 5' probe. (C) RNA blot analysis of 10 μ g of total RNA isolated from E12.5 embryonic fibroblasts and probed with the *Atox1* or 18S (Ambion) DNA probe. (D) Immunoblot analysis of *Atox1* protein in E12.5 embryonic fibroblasts. One-hundred-microgram cell lysates were separated by 10–20% Tricine SDS/PAGE gel and probed with ATOX1 antisera followed by chemiluminescent detection.

2.75%, +/- 40.6 \pm 3.84, -/- 40.13 \pm 2.1%), serum glucose (+/+ 60 \pm 4.58 mg/dl, +/- 47.27 \pm 17.84 mg/dl, -/- 34.5 \pm 7.55 mg/dl), and electrolyte values (sodium; +/+ 143 \pm 1.73 mmol/liter, +/- 141.53 \pm 4.85 mmol/liter, -/- 140.25 \pm 0.96 mmol/liter), in comparison with wt littermates, P3 *Atox1*^{-/-} pups displayed decreased activity and considerable mortality (Fig. 2B). Despite the trend toward lower serum glucose values in *Atox1*^{-/-} pups, these values were within the normal range observed in newborn mice. *Atox1*^{-/-} pups displayed skin laxity, and some animals exhibited peripartum hemorrhaging, which contributed to the overall early mortality (Fig. 2C and D). Genotyping of a total of 166 progeny from *Atox1*^{+/-} intercrosses identified 49 *Atox1*^{-/-} pups, of which 33 survived beyond P3. Before weaning, an additional six animals died from prolonged seizure activity, giving an overall perinatal mortality of 45%. Unlike the *Atox1*^{-/-} mice, the growth, mortality, and gross phenotype of *Atox1*^{+/-} mice were found to be indistinguishable from their wt littermates (data not shown). Beyond weaning, surviving *Atox1*^{-/-} mice remained growth-retarded, hypothermic, and hypopigmented (Fig. 2E), suggesting long-term effects of perinatal *Atox1* deficiency.

The phenotypes observed in *Atox1*^{-/-} animals were in part similar to phenotypes observed in copper-deprived animals, indicating that perinatal copper homeostasis may be perturbed in the absence of *Atox1*. To examine copper homeostasis in *Atox1*^{-/-} mice, ^{64}Cu was administered intravenously to pregnant females from *Atox1*^{+/-} intercrosses; 24 h later, the amount of ^{64}Cu distributed in individual placentas and their corresponding embryos was determined. Significantly less copper was transported into *Atox1*^{-/-} embryos as compared with *Atox1*^{+/+} and *Atox1*^{+/-} embryos. Most of the copper in the *Atox1*^{-/-} fetuses remained in the placenta (Fig. 3A). Transplacental nutrient uptake from the maternal circulation is mediated by syncytiotro-

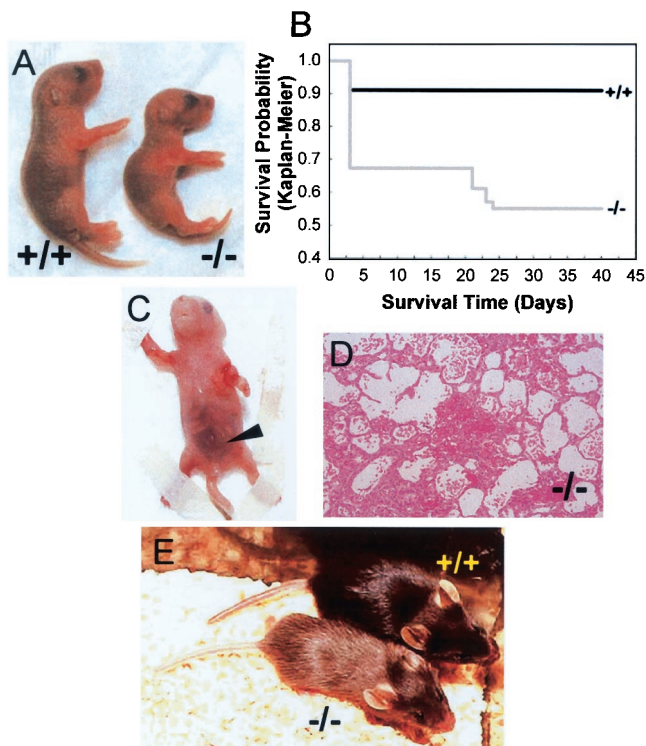


Fig. 2. *Atox1* deficiency results in growth failure and mortality. (A) Images of *Atox1*^{+/+} (Left) and *Atox1*^{-/-} pups (Right) depicting growth differences at P3. (B) Kaplan–Meier plot of survival in progeny from *Atox1*^{+/+} ♂ × *Atox1*^{+/-} ♀ mating ($n = 166$). Note initial drop by P3, followed by another decrease because of seizures around weaning age. Abdominal hemorrhage (arrowhead) (C) and micrograph (100×) depicting pulmonary alveolar hemorrhage (D) observed in some *Atox1*^{-/-} newborn pups. (E) Twenty-three-day-old weanling *Atox1*^{+/+} (Right) and *Atox1*^{-/-} (Left) mice. Note size difference and the hypopigmentation of tail and coat color.

phoblasts and capillary endothelium cells, which are embryonic in origin and line the maternal blood vessels within the placenta. Because the aberration in placental copper transport corresponds specifically to *Atox1*^{-/-} genotype, the data suggest that *Atox1*-deficient cells are unable to maintain normal copper status from maternally derived nutrients. To test this hypothesis, MEFs isolated from E12.5 embryos were incubated with ⁶⁴Cu containing media, and the total amount of copper remaining within the cells was determined after 68 h. *Atox1*^{-/-} MEFs retained significantly greater amounts of copper compared with cells derived from *Atox1*^{+/+} or *Atox1*^{+/-} littermates. A similar phenotype of copper retention was observed when these studies were repeated with fibroblasts that were deficient in the Menkes ATPase (Fig. 3B) (21). The difference in the amount of copper accumulated by the Menkes and *Atox1*^{-/-} fibroblasts may be because of genetic strain differences or may reflect the fact that the Menkes (*Mo*^{br-j}) defect results in a partial loss-of-function of this protein. The increase in copper accumulation within *Atox1*^{-/-} cells was not because of differences in copper uptake, as the initial rate for copper uptake was identical in wt and *Atox1*^{-/-} MEFs (Fig. 3C). To further characterize the copper-retaining phenotype of *Atox1*^{-/-} cells, MEFs were pulse labeled with ⁶⁴Cu for 1 h, and cells were analyzed at specific chase periods for ⁶⁴Cu retained. *Atox1*-deficient MEFs revealed a severe impairment in copper efflux compared with wt cells. Thus, *Atox1*^{-/-} cells accumulate copper because of defective copper efflux from the cell (Fig. 3D).

A reduction in placental copper transport should result in newborn mice with decreased copper content in biosynthetically

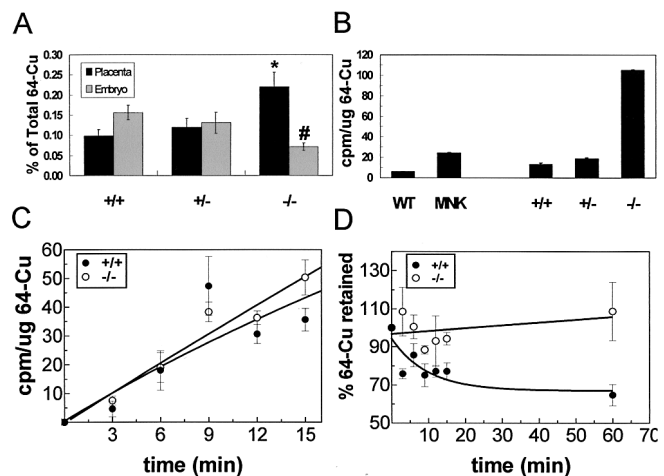


Fig. 3. *Atox1* is essential for normal copper homeostasis. (A) Placental copper transport was determined in E14.5 pregnant females from *Atox1*^{+/-} ♂ × *Atox1*^{+/-} ♀ mating. Fifty micrograms of ⁶⁴Cu was injected intravenously into pregnant dams, and 24 h later the placenta and embryo were dissected from maternal tissue and ⁶⁴Cu incorporation quantified in a gamma counter. Data represent the mean ± SEM from four separate litters and at least 10 animals of each genotype. Each data point is calculated as the amount of ⁶⁴Cu retained by the tissue relative to the total amount of ⁶⁴Cu injected into the mother (*, $P < 0.05$ among the *+/+* and *-/-* placenta and *+/+* and *-/-* embryos; #, $P < 0.01$ between *-/-* placenta and *-/-* embryos; P values were calculated by using a one-way ANOVA with Student–Newman–Keuls multiple comparison test). (B) ⁶⁴Cu retention was determined in cultured fibroblasts derived from *Atox1* mouse embryos (E12.4 *+/+*, *+/-*, and *-/-*) or mouse cell lines (wt, 802–5; MNK, 802–1). Cells (2×10^5) were incubated with 8×10^6 cpm of ⁶⁴Cu. After 68 h, the cells were washed, lysed, and analyzed for ⁶⁴Cu retained by using a gamma counter. Each data point represents the mean ± SEM from three separate experiments performed in triplicate and expressed as cpm/μg of total cell protein. Copper uptake (C) and copper efflux (D) were performed by incubating MEFs with 200 nM ⁶⁴Cu per 4×10^4 cells. For efflux, cells were pulsed with ⁶⁴Cu for 1 h followed by several chase periods with unsupplemented culture media. Cells were harvested at time intervals indicated and processed as described above.

active tissues such as the neonatal liver and brain. Consistent with this concept, P2 *Atox1*^{-/-} pups had 50% less copper in the liver (mean ± SD: *+/+*, 20.2 ± 4.12 μg/g; *-/-*, 10.1 ± 1.71 μg/g, $P < 0.01$) and in the brain (*+/+*, 1.37 ± 0.35 μg/g; *-/-*, 0.685 ± 0.174 μg/g, $P < 0.01$). Furthermore, the activity of essential cupro-enzymes including brain cytochrome oxidase (COX; *+/+*, 0.42 ± 0.02 unit/mg; *-/-*, 0.267 ± 0.03 unit/mg, $P < 0.01$) and tyrosinase (skin tissue from *-/-* pups showed ≈25% of tyrosinase activity compared with *+/+* littermates) was significantly decreased in P2 *Atox1*^{-/-} mice. The diminution in brain COX activity was not because of differences in mitochondrial number or integrity, as the activity of the inner mitochondrial membrane protein, succinate dehydrogenase, was normal (*+/+*, 0.013 ± 0.002 unit/mg, *-/-*, 0.014 ± 0.003 unit/mg).

As placental transfer of nutrients is often dependent on both maternal and fetal components, progeny from *Atox1*^{+/-} ♂ × *Atox1*^{-/-} ♀ and *Atox1*^{-/-} ♂ × *Atox1*^{+/-} ♀ intercrosses were examined. *Atox1*^{-/-} mice derived from *Atox1*^{-/-} mothers exhibited a striking phenotype of growth retardation, skin laxity, and hypopigmentation as compared with its *Atox1*^{+/-} littermates (Fig. 4A). The phenotype in these *Atox1*^{-/-} mice was more severe than that observed previously in *Atox1*^{-/-} mice derived from heterozygote mothers, as evidenced by a near complete lack of tyrosinase enzyme activity in skin tissue (Fig. 4B), despite the presence of normal amounts of tyrosinase protein in those

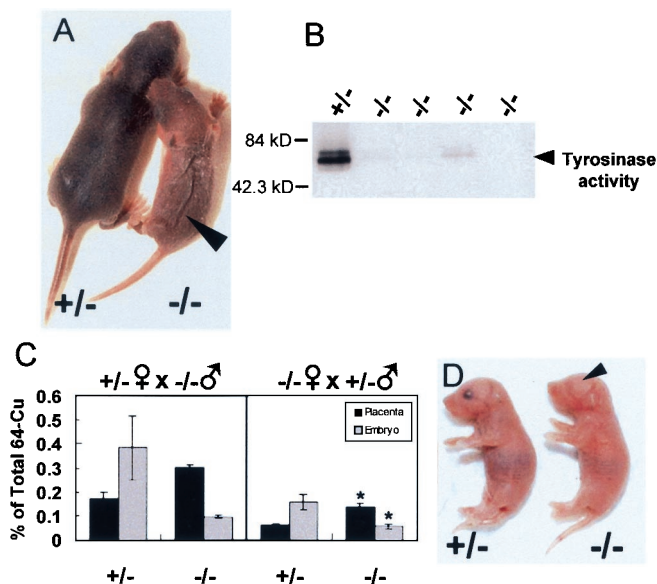


Fig. 4. *Atox1*^{-/-} progeny exhibit a maternal effect. (A) Images of *Atox1*^{+/-} (Left) and *Atox1*^{-/-} (Right) P8 pups from *Atox1*^{+/-} ♂ × *Atox1*^{-/-} ♀ mating. Note skin laxity on the dorsal surface (arrowhead), hypopigmentation, and growth retardation (body weight: +/− = 3.31 g, −/− = 1.74 g). (B) Tyrosinase activity was determined in 100 μg of skin tissue extract separated on a 4–20% SDS/PAGE gel and assayed for dopa oxidase activity. Each lane represents a P8 skin sample from *Atox1*^{+/-} ♂ × *Atox1*^{-/-} ♀ progeny. (C) Placental copper transport was determined in *Atox1*^{+/-} and *Atox1*^{-/-} pregnant females mated to the indicated males. Data represent the mean ± SEM from three separate litters and at least four animals of each genotype (*, *P* < 0.01 for −/− placentas and −/− embryos derived from *Atox1*^{+/-} versus *Atox1*^{-/-} mothers). (D) Image of *Atox1*^{-/-} P2 pup showing microphthalmia (Left) and *Atox1*^{+/-} littermate (Right) from *Atox1*^{+/-} ♂ × *Atox1*^{-/-} ♀ mating.

samples (data not shown). *Atox1*^{-/-} pups showed increased mortality within the first day of life. Six *Atox1*^{-/-} pups (46%) died within 24 h after birth from *Atox1*^{+/-} ♂ × *Atox1*^{-/-} ♀ mating (three litters; 13 −/−, 12 +/−), whereas two *Atox1*^{-/-} pups (20%) died within that time period from *Atox1*^{-/-} ♂ × *Atox1*^{+/-} ♀ mating (three litters; 10 −/−, 10 +/−). These findings suggest an influence of maternal *Atox1* deficiency on perinatal copper metabolism, which, although not sufficient to result in overt signs or symptoms in *Atox1*^{+/-} pups (Fig. 4A), significantly exacerbated the copper deficiency in *Atox1*^{-/-} pups. The concept of maternal *Atox1* influence was supported by placental copper transport studies. As noted previously in Fig. 3A, the difference in ⁶⁴Cu distribution between the placenta and embryo was found to be dependent on the embryonic genotype (Fig. 4C). However, now an overall reduction of 60% in copper availability for placental transport was observed in *Atox1*^{-/-} fetuses derived from *Atox1*^{-/-} mothers compared with *Atox1*^{-/-} fetuses derived from *Atox1*^{+/-} mothers (Fig. 4C). Furthermore, some *Atox1*^{-/-} pups born to *Atox1*^{-/-} mothers demonstrated severe congenital eye defects (Fig. 4D). Microphthalmia was observed in six *Atox1*^{-/-} pups obtained from *Atox1*^{+/-} ♂ × *Atox1*^{-/-} ♀ mating (11 litters, 68 pups), of which only one mouse survived past P3. This phenotype was not due to the mouse genetic background because *Atox1*^{-/-} progeny from the same number of litters from *Atox1*^{-/-} ♂ × *Atox1*^{+/-} ♀ and *Atox1*^{+/-} ♂ × *Atox1*^{+/-} ♀ mating did not show microphthalmia. In addition, occasional *Atox1*^{-/-} mice born to *Atox1*^{-/-} mothers also demonstrated central nervous system malformations and other developmental abnormalities not observed in control littermates.

Discussion

The data in this study demonstrate a critical role for the metallochaperone ATOX1 in mammalian copper homeostasis. The striking phenotypes observed in *Atox1*^{-/-} mice are in part similar to those observed in copper-deprived animals where diminished activity of the cupro-enzymes lysyl oxidase, dopamine monoxygenase, and tyrosinase results in impaired connective tissue integrity, temperature regulation, and pigment formation (1, 2). The copper-retaining phenotype of *Atox1*-deficient MEFs reveals the cellular mechanism underlying the impaired placental copper transfer to *Atox1*^{-/-} embryos, where copper retention within the placenta, due to defective cellular copper efflux, results in decreased copper availability for the fetal circulation. These data, taken together with the demonstrated interaction between ATOX1 and the copper-transporting ATPases (9, 10), definitively reveal a role for ATOX1 in the pathway of copper trafficking from the cytoplasm to the secretory pathway in mammalian cells.

The seizures, hypothermia, and neurodegeneration observed in humans with Menkes disease, and in mice with mutations at the homologous mottled locus, have been attributed to regional alterations of COX activity secondary to copper deficiency in the neonatal brain (17, 22). Thus, it is reasonable to assume that the morbidity associated with *Atox1*-deficient mice is in part related to reduced COX activity in specific areas of the brain that are metabolically active during development. Importantly, previous observations of the phenotype of different mottled alleles (*Mo*) have demonstrated a correlation between the type and severity of symptoms and the amount of *in utero* copper transferred to the developing fetus (23). For example, *dappled* mice (*Mo*^{dp}) die *in utero* from impaired connective tissue integrity and hemorrhage secondary to a deficiency in lysyl oxidase activity, whereas *brindled* mice (*Mo*^{br}) have increased but variable neonatal mortality similar to that observed here in the *Atox1*^{-/-} mice. The heterogeneity in the phenotype in *Atox1*^{-/-} mice may potentially arise from incomplete penetrance resulting from either specific modifying genetic loci or epigenetic effects such as the amount of perinatal copper available during embryonic growth and development. The latter possibility then reveals phenotypic differences based on developmental and tissue-specific thresholds for copper requirement, a concept reinforced by data from *Ctr1*-deficient animals in the accompanying article (24).

The finding that *Atox1*^{-/-} mice derived from *Atox1*^{-/-} mothers exhibited a more severe phenotype suggests that, in part, copper deficiency in *Atox1*^{-/-} mothers along with *Atox1* deficiency in both maternal and fetal components within the placenta leads to a more acute deprivation of perinatal copper availability to the developing embryo, thus compounding the *Atox1*^{-/-} phenotype. Accordingly, these animals showed a marked impairment in growth, higher mortality, reduced pigmentation because of little or no tyrosinase activity, and microphthalmia. Although the precise role of *Atox1* in eye development is unclear, a similar phenotype of hypopigmentation and microphthalmia is observed in mice deficient in *Mitf*, a transcription factor required for the development and maturation of the neural crest-derived melanocytes (25). These findings then raise the possibility that copper-trafficking pathways involving *Atox1* may play a role in the complex signal transduction events involved in neural crest cell development.

Our findings, together with previous biochemical studies (9, 10), are consistent with the hypothesis that ATOX1 is required for copper trafficking to the secretory pathway of mammalian cells through interaction with the Menkes and Wilson ATPase. Thus, the severe pleiotropic phenotype in *Atox1* deficiency may be because of impaired *in utero* copper delivery to both the Menkes and Wilson proteins during development. Furthermore, *Atox1* may have additional roles during cell differentiation and

survival, a concept supported by recent studies implicating a direct role for Atox1 in copper-dependent antioxidant and apoptotic defense in neurons (26). The ability of excess copper to partially compensate for Atox1 deficiency in yeast (6) suggests that the phenotype observed in Atox1-deficient mice might also be affected by alterations in available copper. Preliminary studies administering i.p. copper to neonatal mice and weanling mice support this concept in that these animals demonstrate an improvement in survival and rescue of coat color. The microphthalmia and other developmental defects associated with Atox1 deficiency, and the embryonic lethality associated with loss of Ctr1 in the accompanying report (24), reiterate the essential role for copper in fetal development. Current efforts are now focused on careful delineation of Atox1-associated phenotypes during tissue morphogenesis. In this regard, these studies underscore the unique potential of genetic models to contribute new knowledge to our understanding of the complex relationship between

nutrition and fetal development. The observation that maternal genotype may contribute to differences in fetal copper acquisition and fetal development highlights an important complexity in considering genetic and environmental influences on nutrient delivery to the developing fetus. As such, the approach presented here provides a useful heuristic paradigm for defining the role of specific nutrients in the pathogenesis of birth defects, an area recently highlighted by the discovery of the role of folic acid in human fetal neural tube closure (27).

We thank Dennis Thiele for sharing information before publication, Michael Welch for ^{64}Cu , and Scott Saunders, Lou Muglia, and Dave Wilson for helpful discussions and critical review of the manuscript. This work was supported by National Institutes of Health Postdoctoral Fellowship HL07873 (to I.H.) and National Institutes of Health Research Grant DK58783 (to J.D.G.). J.D.G. is a recipient of the Burroughs Wellcome Scholar Award in Experimental Therapeutics.

1. Pena, M. M., Lee, J. & Thiele, D. J. (1999) *J. Nutr.* **129**, 1251–1260.
2. Culotta, V. C. & Gitlin, J. D. (2001) in *The Metabolic and Molecular Bases of Inherited Diseases*, eds. Scriver, C. R., Beaudet, A. L., Sly, W. S. & Valle, D. (McGraw-Hill, New York), Vol. 2, pp. 3105–3126.
3. Valentine, J. & Gralla, E. B. (1997) *Science* **278**, 817–818.
4. O'Halloran, T. V. & Culotta, V. C. (2000) *J. Biol. Chem.* **275**, 25057–25060.
5. Rae, T. D., Schmidt, P. J., Pufahl, R. A., Culotta, V. C. & O'Halloran, T. V. (1999) *Science* **284**, 805–808.
6. Lin, S. J., Pufahl, R. A., Dancis, A., O'Halloran, T. V. & Culotta, V. C. (1997) *J. Biol. Chem.* **272**, 9215–9220.
7. Pufahl, R. A., Singer, C. P., Peariso, K. L., Lin, S. J., Schmidt, P. J., Fahrni, C. J., Culotta, V. C., Penner-Hahn, J. E. & O'Halloran, T. V. (1997) *Science* **278**, 853–856.
8. Rosenzweig, A. C., Huffman, D. L., Hou, M. Y., Wernimont, A. K., Pufahl, R. A. & O'Halloran, T. V. (1999) *Struct. Fold Des.* **7**, 605–617.
9. Larin, D., Mekios, C., Das, K., Ross, B., Yang, A. S. & Gilliam, T. C. (1999) *J. Biol. Chem.* **274**, 28497–28504.
10. Hamza, I., Schaefer, M., Klomp, L. W. & Gitlin, J. D. (1999) *Proc. Natl. Acad. Sci. USA* **96**, 13363–13368.
11. Faisst, A. M. & Gruss, P. (1998) *Dev. Dyn.* **212**, 293–303.
12. Hamza, I., Klomp, L. W., Gaedigk, R., White, R. A. & Gitlin, J. D. (2000) *Genomics* **63**, 294–297.
13. Gitlin, D., Hughes, W. L. & Janeway, C. A. (1960) *Nature (London)* **188**, 150–151.
14. Mann, J. R., Camakaris, J. & Danks, D. M. (1980) *Biochem. J.* **186**, 629–631.
15. Spector, D. L., Goldman, R. D. & Leinwand, L. A. (1998) *Cells: A Laboratory Manual* (Cold Spring Harbor Lab. Press, Plainview, NY).
16. Kelly, E. J. & Palmiter, R. D. (1996) *Nat. Genet.* **13**, 219–222.
17. Prohaska, J. R. (1983) *J. Nutr.* **113**, 2048–2058.
18. Orlow, S., Lamoreux, M., Pifko-Hirst, S. & Zhou, B. (1993) *J. Invest. Dermatol.* **101**, 137–140.
19. Cooney, G. J., Taegtmeier, H. & Newsholme, E. A. (1981) *Biochem. J.* **200**, 701–703.
20. Bonaldo, P., Chowdhury, K., Stoykova, A., Torres, M. & Gruss, P. (1998) *Exp. Cell Res.* **244**, 125–136.
21. Camakaris, J., Danks, D. M., Ackland, L., Cartwright, E., Borger, P. & Cotton, R. G. (1980) *Biochem. Genet.* **18**, 117–131.
22. Prohaska, J. R. (2000) *Nutrition* **16**, 502–504.
23. Mercer, J. F. (1998) *Am. J. Clin. Nutr.* **67**, 1022S–1028S.
24. Lee, J., Prohaska, J. R. & Thiele, D. J. (2001) *Proc. Natl. Acad. Sci. USA* **98**, 6842–6847.
25. Goding, C. R. (2000) *Genes Dev.* **14**, 1712–1728.
26. Kelner, G. S., Lee, M., Clark, M. E., Maciejewski, D., McGrath, D., Rabizadeh, S., Lyons, T., Bredesen, D., Jenner, P. & Maki, R. A. (2000) *J. Biol. Chem.* **275**, 580–584.
27. Butterworth, C. & Bendich, A. (1996) *Annu. Rev. Nutr.* **16**, 73–97.